Functional expression of the plant alternative oxidase affects growth of the yeast Schizosaccharomyces pombe.

Affourtit, C.; Albury, M.S.; Krab, K.; Moore, A.L.

published in
Journal of Biological Chemistry
1999

DOI (link to publisher)
10.1074/jbc.274.10.6212

document version
Publisher's PDF, also known as Version of record

THE JOURNAL OF BIOLOGICAL CHEMISTRY
Vol. 274, No. 10, Issue of March 5, pp. 6212–6218, 1999

Printed in U.S.A.

Functional Expression of the Plant Alternative Oxidase Affects Growth of the Yeast *Schizosaccharomyces pombe**

(Received for publication, September 29, 1998, and in revised form, December 18, 1998)

Charles Affourtit‡, Mary S. Albury, Klaas Krab§, and Anthony L. Moore¶

From the Department of Biochemistry, School of Biological Sciences, University of Sussex, Falmer, Brighton BN1 9QG, United Kingdom and the §IMBW Section Microbiology, Vrije Universiteit, De Boelelaan 1087, 1081 HV Amsterdam, The Netherlands

We have investigated the extent to which functional expression of the plant alternative oxidase (from *Sauromatum guttatum*) in *Schizosaccharomyces pombe* affects yeast growth. When cells are cultured on glycerol, the maximum specific growth rate is decreased from 0.13 to 0.11 h^{-1} while growth yield is lowered by 20% (from 1.14×10^8 to 9.12×10^7 cells ml^{-1}). Kinetic studies suggest that the effect on growth is mitochondrial in origin. In isolated mitochondria we found that the alternative oxidase actively competes with the cytochrome pathway for reducing equivalents and contributes up to 24% to the overall respiratory activity. Metabolic control analysis reveals that the alternative oxidase exerts a considerable degree of control (22%) on total electron flux. Furthermore, the negative control exerted by the alternative oxidase on the flux ratio of electrons through the cytochrome and alternative pathways is comparable with the positive control exerted on this flux-ratio by the cytochrome pathway. To our knowledge, this is the first paper to report a phenotypic effect because of plant alternative oxidase expression. We suggest that the effect on growth is the result of high engagement of the non-protonmotive alternative oxidase in yeast respiration that, consequently, lowers the efficiency of energy conservation and hence growth.

In addition to a cytochrome *c* oxidase, plant mitochondria contain a cyanide- and antimycin-resistant alternative oxidase that catalyzes the reduction of molecular oxygen to water upon oxidation of ubiquinol (1–5). Alternative oxidase activity is regulated by the reduction level of the Q-pool[1] (6–9) that is a result of the kinetic interplay between the quinone-reducing and quinol-oxidizing enzymes (9). Additional regulatory factors include the mitochondrial concentration of α-keto acids (10) and the redox status of the sulfhydryl/disulfide system (11). The isolation of cDNA clones from several plant and fungal species (for review see Ref. 2) has considerably improved our understanding of the molecular nature of the oxidase. Scrutiny of cDNA-deduced amino acid sequences has resulted in a model of the catalytic site of the protein that has been postulated to contain a coupled binuclear iron center (12, 13). Recent work in our laboratory has resulted in the functional expression of the alternative oxidase (from *Sauromatum guttatum*) in the yeast *Schizosaccharomyces pombe* (14), a system that has been used to study structure-function relations of the alternative oxidase by site-directed mutagenesis (15).

The plant alternative oxidase is non-protonmotive (16, 17), suggesting that any contribution of the enzyme to the overall respiratory activity would affect the efficiency of mitochondrial energy metabolism in plants. Although constitutive overexpression or silencing of the alternative oxidase protein in tobacco and potato has been shown to affect mitochondrial respiration (18, 19), it has not been shown to alter the characteristics of plant growth. The functional expression of the alternative oxidase in *S. pombe* (14) has raised the question as to whether or not the mitochondrial respiratory kinetics and growth of this yeast are affected by the constitutive presence of the oxidase.

Relatively few studies have been performed to characterize the mitochondrial respiratory kinetics of *S. pombe* (20, 21). However, the presence of at least two substrate dehydrogenases is evident as both added NADH and succinate are readily oxidized in isolated mitochondria (20, 21). The exhibited respiratory activity is fully sensitive to antimycin and myxothiazol and is linearly dependent upon the Q-redox poise (20), suggesting that the respiratory chain does not branch at the level of the Q-pool.

Heterologous expression of the plant alternative oxidase establishes cyanide-insensitive mitochondrial respiratory activity in *S. pombe* (14) and thereby introduces an additional oxygen-reducing pathway. Because of the presence of two oxidases and an external-NADH dehydrogenase, the mitochondrial respiratory chain in this yeast system is comparable with those found in plants. In transformed *S. pombe* cells, functional expression of the alternative oxidase may be fully repressed or induced by including or excluding thiamine in the growth medium, respectively (14). This system therefore provides an excellent model to study effects of the presence of the plant alternative oxidase on growth and mitochondrial respiration.

In the present paper, growth physiology experiments suggest that the functional expression of the alternative oxidase inhibits the growth of *S. pombe* cells, both in terms of growth yield and rate. Kinetic analysis of respiration strongly indicates that these effects on growth are mitochondrial in origin since they reveal that the non-protonmotive alternative oxidase actively competes for reducing equivalents with the cytochrome pathway, contributing up to 24% to the total mitochondrial respiratory activity. MCA reveals that the alternative oxidase has a considerable degree of control on overall electron flux (C^J = 0.22) at the expense of the cytochrome pathway. The calculated control coefficients indicate that the cytochrome route and the alternative oxidase exert comparable control on the relative

* This work was supported by a grant from the Biotechnology and Biological Sciences Research Council. The costs of publication of this article were defrayed in part by the payment of page charges. This article must therefore be hereby marked "*advertisement*" in accordance with 18 U.S.C. Section 1734 solely to indicate this fact.

‡ Recipient of a BBSRC studentship.

¶ To whom correspondence should be addressed. Tel.: 44-1273-678479; Fax: 44-1273-678433; E-mail: a.l.moore@susx.ac.uk.

[1] The abbreviations used are: Q, ubiquinone; CCCP, carbonyl cyanide *m*-chlorophenylhydrazone; MOPS, 3-(*N*-morpholino)propanesulfonic acid; QH_2, reduced ubiquinone; MCA, metabolic control analysis; C^J, flux control coefficient; C^{rca}, flux ratio control coefficient; AOX, alternative oxidase.

fluxes through the respective quinol-oxidizing pathways. Both of these observations confirm the potential of the alternative oxidase to divert reducing equivalents away from the cytochrome pathway, thereby lowering the overall efficiency of energy conservation.

EXPERIMENTAL PROCEDURES

Strains and Growth Conditions—The *S. pombe* strain used was sp.011 (*ade*6–704, *leu*1–32, *ura*4-D18, h^-). Minimal media and growth conditions for both growth and kinetic experiments were as described by Murray *et al.* (22) with the additional inclusion of 2.75 μM $FeCl_3$ and lack of Mn^{2+} and the presence or absence of 0.5 mM thiamine. Growth experiments were performed in minimal medium containing 2% glucose or 3% glycerol with 0.1% glucose.

Yeast Transformation—The construction of plasmid pREP1/AOX that contains the alternative oxidase coding sequence under control of the *nmt*1 promoter has been previously reported by Albury *et al.* (14). *S. pombe* cells were transformed using a modified lithium acetate method (23).

Isolation of Mitochondria—*S. pombe* cells were aerobically grown overnight in 1-liter minimal medium cultures to a density of approximately 5×10^7 cells ml^{-1} (mid-logarithmic phase). Mitochondrial isolation was based on a protocol previously described by Moore *et al.* (20) but without incubation of cells with 0.5 M β-mercaptoethanol nor the subsequent KCl washes and purification of mitochondria on Percoll gradients. Spheroplasts were prepared essentially as described (20) but with modified concentrations: cells ($0.5–1.5 \times 10^9$ ml^{-1}) were incubated at 30 °C for 15 min with 1 mg ml^{-1} Zymolyase and for a further 45 min following the addition of 1 mg ml^{-1} lysing enzymes.

Measurement of Respiratory Kinetics—Respiratory activity and reduction level of the Q-pool were simultaneously measured voltametrically in a specially constructed chamber (University of Sussex) housing a Rank oxygen electrode and glassy carbon and platinum electrodes connected to a Ag/AgCl reference electrode similar to that described by Moore *et al.* (6). Mitochondria (0.5–1.0 mg) were incubated in 2.2-ml reaction medium that contained 0.3 M mannitol, 1 mM $MgCl_2$, 5 mM K_2PO_4 buffer, 10 mM KCl, 20 mM MOPS (pH 7.2), and 1 μM Q-1. Other chemicals specific to the experiment were added as described in the legends of Figs. 2 and 3.

Growth Experiments—Batch cultures (150-ml minimal medium with or without 0.5 mM thiamine and as carbon source either 2% glucose or 3% glycerol with 0.1% glucose) were inoculated from agar plates with transformed (pREP1/AOX) *S. pombe* cells and grown aerobically in an incubator/shaker at 30 °C. Light microscopy revealed that the morphology of cells with and without alternative oxidase was comparable, and therefore light scattering was considered a suitable way to determine cell numbers. At set times, aliquots (2 ml) were taken and diluted, and the optical density was read at 595 nm (A_{595}). Determination of a standard curve revealed that the scattering of light at 595 nm is linearly dependent upon the counted number of *S. pombe* cells ml^{-1} up to A_{595} values of 0.5.

Assays and Reagents—The concentration of mitochondrial protein was estimated using the bicinchoninic acid method with bovine serum albumin as a standard (24). Chemicals were, unless stated otherwise, obtained from Sigma (Poole, Dorset, UK) or ICN Biomedicals, Inc. (Aurora, OH).

Kinetic Modeling and Metabolic Control Analysis—Mitochondria isolated from *S. pombe* cells expressing the alternative oxidase contain a respiratory network that is comparable with those found in plant systems. A relatively easy to use model to describe and predict respiratory kinetics within plant mitochondria has been postulated by Van den Bergen and colleagues (9). We have used this approach, in which both quinone-reducing and quinol-oxidizing enzymes are assumed to exhibit reversible Michaelis-Menten kinetics with respect to Q/QH_2 (sum of substrate and product is constant), to model the kinetic *S. pombe* data presented in this paper. Because this model accounts for total electron flux from respiratory substrate to oxygen, it effectively describes the kinetic behavior of the entire electron transfer system and therefore provides a good starting point to study mitochondrial electron transfer in terms of metabolic control analysis (see Refs. 25 and 26).

The electron transfer system in *S. pombe* mitochondria was studied using a "top-down" approach (26–29), being divided into two quinone-reducing blocks (succinate dehydrogenase with dicarboxylate carrier and external-NADH dehydrogenase) and two quinol-oxidizing blocks (cytochrome pathway and alternative oxidase), all of which are linked by the Q-pool. Hyperbolic fits (9) describing the experimentally derived kinetics of the individual blocks were used to calculate steady state reduction levels of the Q-pool and to derive elasticities of the respective enzyme blocks with respect to QH_2 (27, 28). Flux and flux ratio control coefficients were calculated from the elasticity coefficients using a matrix-based method according to Westerhoff and Kell (30).

RESULTS

The Effect of Alternative Oxidase Expression on Growth Physiology—To investigate whether or not growth characteristics of batch-cultured *S. pombe* were affected by the expression of the non-protonmotive alternative oxidase, growth curves were determined using cells transformed with pREP1/AOX grown on either a fermentable or non-fermentable carbon source in the presence or absence of thiamine (Fig. 1). The results presented in Fig. 1*A* indicate that growth of *S. pombe* on glucose is not affected by the presence of the alternative oxidase since the growth yield in the absence or the presence of the oxidase is the same ($\sim 1.3 \times 10^8$ cells ml^{-1}). However, a semi-logarithmic representation of these data (Fig. 1*B*) reveals a small difference in growth rate during log phase with cells expressing the oxidase exhibiting a 12% lower rate than control cells (0.167 instead of 0.190 h^{-1}). The decrease in growth rate during (early) exponential phase is more pronounced (18%) when cells are grown on glycerol (from 0.131 to 0.108 h^{-1}, Fig. 1*D*). The growth curve presented in Fig. 1*C* clearly shows that under the latter conditions, when the yeast has to rely predominantly on mitochondrial respiration to produce ATP, the expression of the alternative oxidase has an additional effect on the growth yield that is lowered by 20% (from 1.14×10^8 to 9.12×10^7 cells ml^{-1}).

To confirm that these effects on growth yield and rate could be specifically attributed to the expression of the alternative oxidase and were not because of a thiamine limitation, similar growth studies were performed using cells transformed with pREP1 only (*i.e.* a plasmid lacking the alternative oxidase gene). No differences could be observed between cells grown in the absence or the presence of thiamine (data not shown).

The Effect of Alternative Oxidase Expression on Mitochondrial Respiratory Kinetics—The results presented above indicate that the growth physiology of *S. pombe* is negatively affected by the expression of a single gene encoding the plant alternative oxidase (Fig. 1). These results strongly suggest that the observed effects on growth might be because of an effect on mitochondrial respiration. We therefore investigated respiratory kinetics in mitochondria isolated from cells in which the expression of the alternative oxidase was either induced or repressed.

The dependence of electron flow through quinol-oxidizing pathways upon the reduction level of the Q-pool was determined by titrating respiratory activity with malonate in a variety of respiratory states (6–9); the results of these experiments are summarized in Fig. 2. In cells not expressing the alternative oxidase, electron flow through the cytochrome pathway under state 4 conditions is approximately linearly dependent upon the Q-redox poise (Fig. 2*A*). Addition of ADP induces a subtle change in this kinetic behavior that is reflected by stimulated electron transfer rates at high (>80%) Q-reduction levels only. Uncoupling with CCCP results in a more significant increase in oxygen uptake rates than in state 3, but again, this occurs exclusively at these high reduction levels of the Q-pool (Fig. 2*A*). Consequently, in *S. pombe* mitochondria the kinetic behavior of the cytochrome pathway with respect to Q/QH_2 under both state 3 and uncoupled conditions is concave. These kinetics are different from those found in any plant system studied to date (*cf.* Ref. 31).

The data depicted in Fig. 2*B* represent experiments performed using mitochondria possessing the alternative oxidase. Fig. 2*B* indicates that electron transfer through the alternative

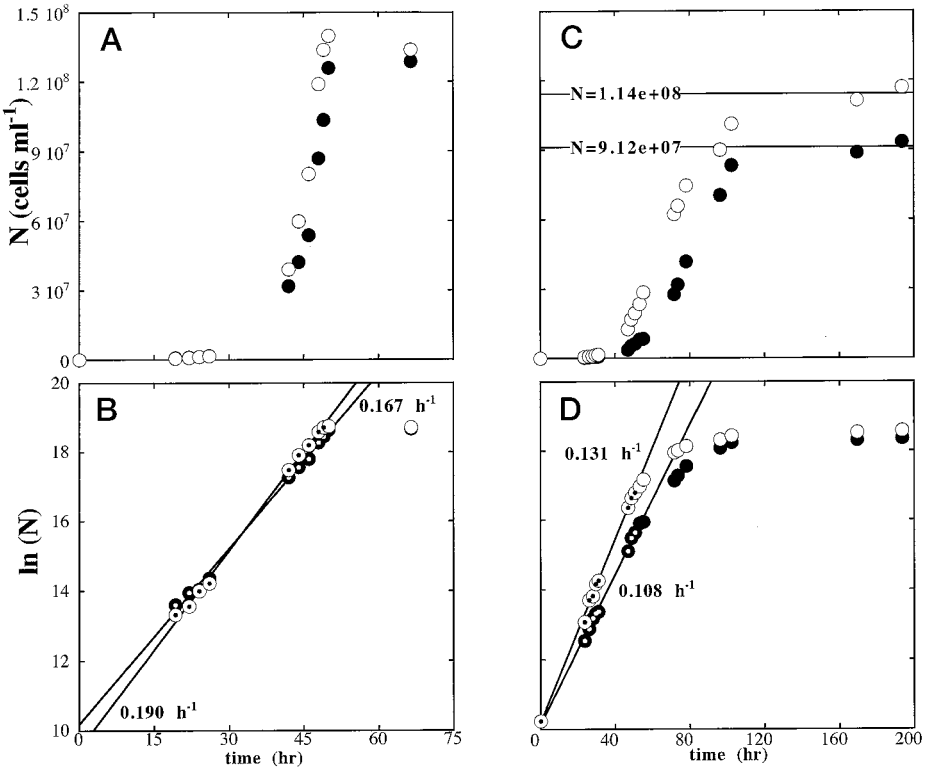

FIG. 1. **Effect of plant alternative oxidase expression on growth characteristics of *S. pombe*.** Cells transformed with pREP1/AOX were grown in the presence or absence of 0.5 mM thiamine in minimal media with 2% glucose (*A* and *B*) or 3% glycerol with 0.1% glucose (*C* and *D*) as the sole carbon source. As described under "Experimental Procedures," cell densities were calculated from A_{595} values (4–5 for each data point) that varied less than 3%. Typical experiments (repeated at least twice) are presented showing growth curves of cells in which expression of the alternative oxidase was repressed (○) or induced (●). *Dotted* data points in the semi-logarithmic plots were fitted using linear equations. Numbers refer to growth yield (*C*) or maximum specific growth rate (*B* and *D*).

oxidase commences when the Q-pool is approximately 20% reduced and that this flow increases disproportionally upon an increasing Q-redox poise. Activity at such a low Q-reduction level suggests that the relative affinity of the alternative oxidase for QH_2 is high compared with that found in plants (when the alternative oxidase has not been activated) and indicates that the oxidase has the potential to compete for electrons with the cytochrome pathway (10). A direct comparison of cytochrome pathway kinetics (Fig. 2*C*) reveals that electron flow through the cytochrome route under state 4 and state 3 conditions is diminished by expression of the alternative oxidase, particularly at Q-reduction levels higher than 30%, whereas electron transfer under uncoupled conditions is not affected significantly at any Q-reduction level. This is illustrated by the kinetics of the overall oxygen uptake which show that, under state 4 and state 3 conditions, oxygen uptake rates are higher at comparable reduction levels in mitochondria lacking the alternative oxidase (Fig. 2*A*) than in mitochondria possessing the enzyme (Fig. 2*B*). Under uncoupled conditions, the kinetics are comparable in both types.

The kinetics of quinol-oxidizing pathways should be independent of the source of reducing equivalents *i.e.* the type of substrate. The data represented by the *insets* of Fig. 2, *A* and *B* were obtained during succinate-oxidation in the absence of malonate and also include steady states achieved upon oxidation of added NADH under different energetic conditions (see steady states 6–9). It is clear that the latter steady states can be readily described by the appropriate curves fitted through data obtained by malonate titrations. This indicates that the quinol-oxidizing pathways are indeed kinetically independent of the employed quinone-reducing enzyme(s), both in cells with and without alternative oxidase. A second point to be addressed with respect to the *insets* of Fig. 2 concerns succinate dehydrogenase which, as is the case in many mammalian (32) and plant mitochondria (33), requires activation. In *S. pombe*, activation is ensured by including ATP and glutamate (to remove any bound oxaloacetate by transamination) in the reaction mixture (20). From the *insets* of Fig. 2, it can be seen that the steady states reached in the absence of glutamate and/or ATP (see steady states 1 and 2) fit well on the curves describing the overall state 4 kinetics of Q-oxidizing routes, confirming that it is indeed the activation of succinate dehydrogenase that is responsible for increased respiratory activity and not a stimulation of the cytochrome or alternative pathway. Finally, the steady states achieved in the presence of antimycin A (see steady state 9) confirm that the alternative oxidase is either absent (Fig. 2*A*, *inset*) or present (Fig. 2*B*, *inset*), respectively, in mitochondria isolated from cells grown in medium containing or lacking thiamine. Antimycin-insensitive respiratory activity (steady state 9 in Fig. 2*B*, *inset*) was fully inhibited by octyl-gallate (data not shown), a potent specific inhibitor of the alternative oxidase (34).

The dependence of electron transfer through quinone-reducing enzymes upon the reduction level of the Q-pool was determined by titrating the oxidation rates of succinate or NADH with antimycin A (9). The data shown in Fig. 3 reveal that the expression of the alternative oxidase does not have a significant effect on the kinetic behavior, under state 4 conditions, of either succinate dehydrogenase (Fig. 3*A*) or the external-NADH dehydrogenase (Fig. 3*B*). The *insets* of Fig. 3 show respiratory steady states that are unaffected by antimycin A and were achieved during succinate- or NADH-oxidation under state 4, state 3, and uncoupled conditions in the presence or the absence of the alternative oxidase. An effect of the protonmotive force upon kinetics of non-protonmotive quinone-reducing pathways would not be anticipated. It is clear, however, that addition of ADP or CCCP to mitochondria lacking the alternative oxidase results in steady states (see steady states 3 and 5 in *insets*, respectively) that cannot be described by the fits of state 4 kinetics of succinate (Fig. 3*A*, *inset*) and external-NADH dehydrogenase (Fig. 3*B*, *inset*). The reason for the lack of fit is, at present, unclear.

Kinetic Modeling and Metabolic Control Analysis—To quantify the effects of the expression of the alternative oxidase on the kinetic behavior of the overall electron transfer system in *S. pombe* mitochondria, experimental data representing the ki-

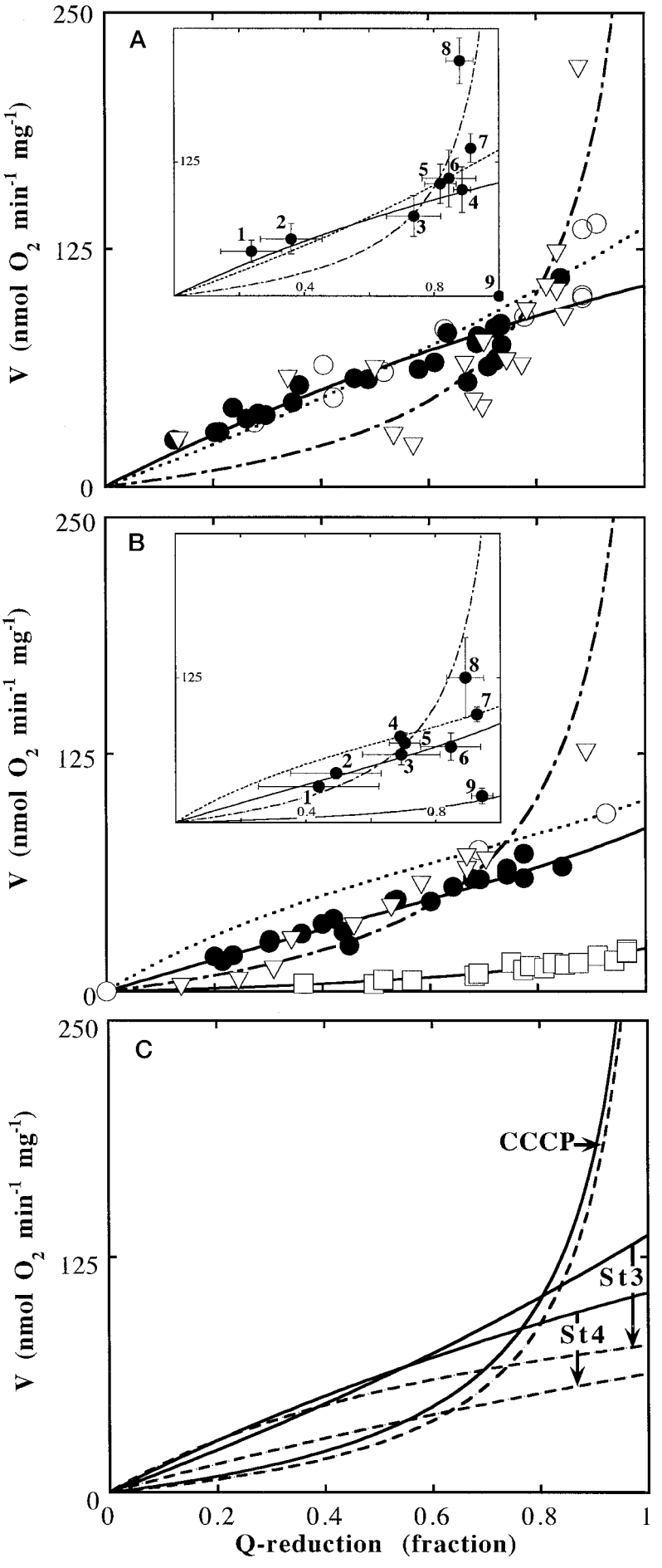

FIG. 2. **Effect of alternative oxidase expression on kinetics of quinol-oxidizing enzymes in *S. pombe* mitochondria.** The dependence of electron flow through quinol-oxidizing pathways upon the reduction level of the Q-pool was determined in mitochondria lacking (*A*) or containing (*B*) the alternative oxidase by titrating the oxidation of 9 mM succinate with 0–9 mM malonate in the presence of 0.2 mM ATP and 9 mM glutamate. Titrations to determine the total Q-oxidizing kinetics in these two types of mitochondria—*i.e.* cytochrome pathway alone (*A*) and sum of cytochrome + alternative pathway (*B*)—were performed under state 4 (●), state 3 (○, 1 mM ADP), and uncoupled conditions (▽, 1 μM CCCP). To reveal the kinetics of the alternative oxidase alone, titrations were performed in the presence of 1.7 μM antimycin A (□). The malonate titrations were obtained from six different mitochondrial preparations, and each set of kinetics is a summation of data from two to four separate respiratory traces. The data shown in the *insets* represent steady states unaffected by malonate and are averages of 5–26 respiratory traces from ten separate mitochondrial preparations. Steady states upon oxidation of 9 mM succinate were achieved with substrate alone (1) or in the cumulative presence of 0.2 mM ATP (2), 9 mM glutamate (3), 1 mM ADP (4), and 1 μM CCCP (5). Steady states upon oxidation of 1.8 mM NADH were reached with substrate only (6) or in the presence of 1 mM ADP (7), 1 μM CCCP (8), or 1.7 μM antimycin A (9). Curves were obtained by modeling the data mathematically as described under "Experimental Procedures" and represent total Q-oxidizing kinetics under state 4 (*solid line* through ●), state 3 (*dotted line* through ○), and uncoupled conditions (*dot/dashed line* through ▽) or the alternative oxidase kinetics alone (*solid line* through □). Cytochrome pathway kinetics in mitochondria lacking (*solid lines*) or containing (*dashed lines*) the alternative oxidase are shown in *panel C*. *Solid lines* are modeled data from *panel A*; *dashed lines* were obtained by subtracting the modeled alternative oxidase kinetics from the modeled total Q-oxidizing kinetics shown in *panel B*.

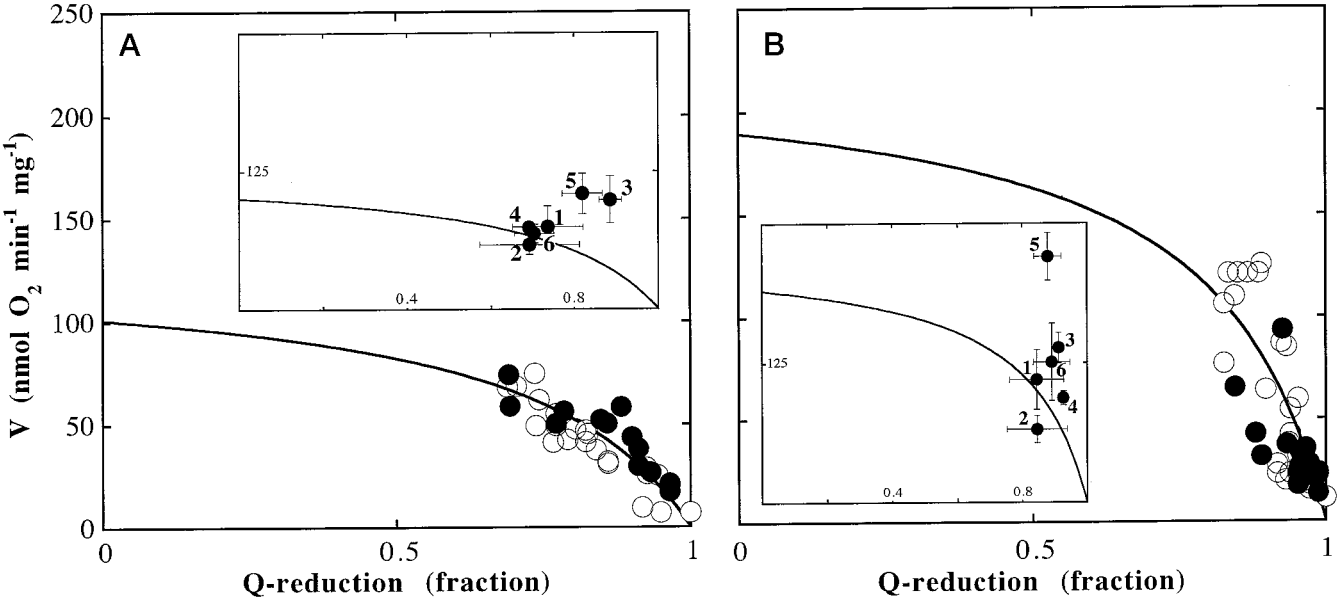

FIG. 3. **Effect of alternative oxidase expression on kinetics of quinone-reducing enzymes in *S. pombe* mitochondria.** The dependence of electron flow through succinate dehydrogenase (*A*) and the external NADH dehydrogenase (*B*) upon the reduction level of the Q-pool was determined in mitochondria lacking (○) or containing (●) the alternative oxidase by titrating the oxidation of 9 mM succinate in the presence of 0.2 mM ATP and 9 mM glutamate (*A*) or the oxidation of 1.8 mM NADH (*B*) with 0–30 nM antimycin A under state 4 conditions. The antimycin A titrations were obtained from three different mitochondrial preparations, and each set of kinetics is a summation of data from two to three separate respiratory traces. The data shown in the *insets* represent steady states unaffected by antimycin A and are averages of 5–24 respiratory traces from ten separate mitochondrial preparations. Steady states were reached upon oxidation of 9 mM succinate + 0.2 mM ATP + 9 mM glutamate (*inset A*) or 1.8 mM NADH (*inset B*) under state 4 (*1* and *2*), state 3 (1 mM ADP; *3* and *4*), or uncoupled conditions (1 μM CCCP; *5* and *6*). Steady states 1, 3, and 5 were reached in mitochondria lacking the alternative oxidase and 2, 4, and 6 in mitochondria containing the oxidase. Combined data in each *panel* were modeled as described under "Experimental Procedures."

netics of both the quinol-oxidizing (Fig. 2) and quinone-reducing (Fig. 3) enzymes were modeled using hyperbolic expressions as described under "Experimental Procedures." The parameters obtained from the mathematical fits were used to calculate Q-reduction levels under different metabolic conditions at which the system reaches a steady state and to calculate the relative contributions of the individual enzymes to the total electron flow. In Fig. 4*A*, fitted data from Figs. 2*B*, 3*A*, and 3*B* have been combined and reveal the kinetic interplay between quinone-reducing and quinol-oxidizing enzymes in mitochondria containing the alternative oxidase. Respiratory steady states are achieved when the electron flow through the reducing pathways equals the flow through oxidizing pathways and are represented by the intersection of the curves describing the kinetics of the respective routes. *In vivo*, it is likely that multiple substrates are oxidized. We have therefore calculated the kinetic parameters for the combined oxidation of succinate and NADH under state 4, state 3, and uncoupled conditions (labeled *A–C* in Fig. 4, respectively) that are tabulated in Fig. 4*B*. Of particular importance are the findings that the alternative oxidase contributes up to 24% of the total electron flow under state 4 conditions and that even under state 3 conditions—likely to reflect the *in vivo* situation most closely—as much as 19% of the overall respiratory activity is accounted for by alternative oxidase activity. Since the alternative oxidase is a non-protonmotive enzyme (16, 17), such a high engagement in respiration is likely to lower the overall efficiency of energy transduction.

The mathematical expressions that we have used to describe the experimentally determined kinetic dependence of each of the respiratory enzymes on the reduction level of the Q-pool (Figs. 2 and 3) provide a good basis to evaluate the effect of alternative oxidase expression on the kinetic behavior of the overall mitochondrial electron transfer system using MCA. The elasticity of the respective enzymes with respect to the Q-redox poise can be directly calculated from the rate equation of the enzyme, its derivative function, and the steady state reduction level of the Q-pool. Control coefficients can then be calculated from the elasticity coefficients using a matrix-based approach (30).

The results presented in Fig. 5 illustrate how the position of the respiratory steady state reached upon the combined state 4 oxidation of succinate and NADH is affected by the presence of the alternative oxidase (Fig. 5*A*). Furthermore, the data quantify how control in these two steady states is distributed among the individual respiratory enzymes (Fig. 5*B*). Although intuitively it is expected that the additional presence of a quinol-oxidizing enzyme should result in an increased flux control (C^J) exerted by the dehydrogenases, it can be seen from Fig. 5*B* that control on total electron flux exerted by the combined activities of succinate and external-NADH dehydrogenase is not significantly affected by the expression of the alternative oxidase (remains ~10%). Interestingly, control exerted by the alternative oxidase on total electron flux is approximately 22%. This appears to be fully at the expense of the control formerly exerted by the cytochrome pathway. The relatively powerful position the alternative oxidase appropriates within the electron transfer system is further illustrated by the degree of control exerted by this oxidase on the ratio of fluxes through both pathways. The negative control exerted by the alternative oxidase on the flux-ratio of electrons through quinol-oxidizing routes is comparable with the positive control exerted on this flux-ratio by the cytochrome pathway (C^{rca} is −0.964 compared with 1.115, Fig. 5*B*).

DISCUSSION

The results described in this paper show that expression of the plant alternative oxidase inhibits the glycerol-dependent growth of the yeast *S. pombe* (Fig. 1, *C* and *D*). It is unlikely that this inhibition is an artifactual effect of heterologous ex-

A

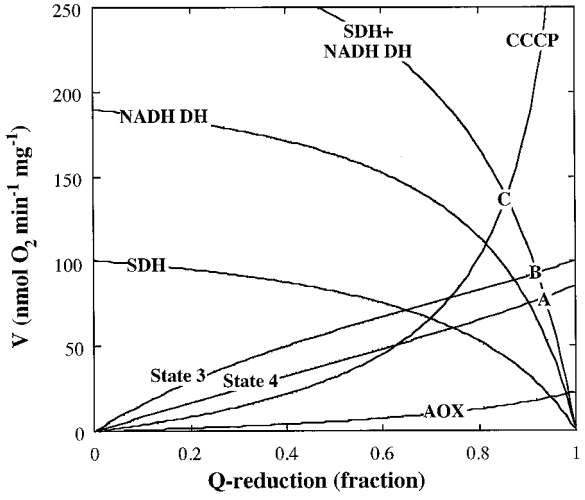

B

steady state	Qr/Qt (%)	V (nmol O_2 min^{-1} mg^{-1})	AOX (%)
state 4 (A)	94	78	24
state 3 (B)	92	93	19
CCCP (C)	86	138	11

FIG. 4. **Kinetic interplay between quinone-reducing and quinol-oxidizing enzymes in *S. pombe* mitochondria containing the alternative oxidase.** Curves representing the kinetics of dehydrogenases and oxidases (*panel A*) were taken from Figs. 2*B*, 3*A*, and 3*B*; the curve representing the combined kinetics of SDH and NADH DH was obtained by addition of the curves describing the individual kinetics of both dehydrogenases. Parameters defining the hyperbolic fits (not shown) were used to calculate the Q-reduction level (Q_r/Q_t), the total rate of electron transfer (*V*), and the contribution of the alternative oxidase to the total electron transfer rate (AOX) upon the combined oxidation of succinate and NADH under state 4, state 3, and uncoupled conditions (*panel B*). *SDH*, succinate dehydrogenase; *NADH DH*, external-NADH dehydrogenase; *AOX*, alternative oxidase.

A

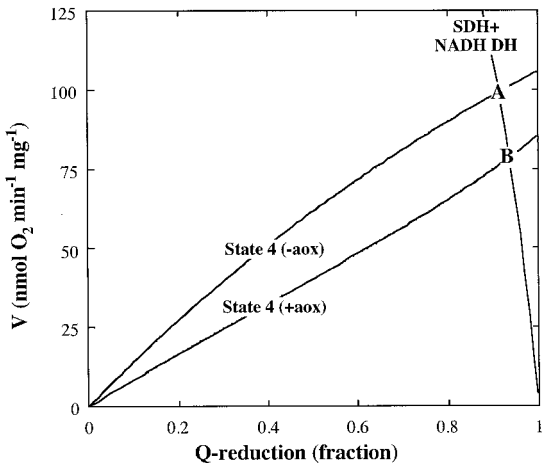

B

steady state	control by:	C^J	C^{rca}
- aox	SDH	0.027	-
state 4	NADH DH	0.062	-
(A)	Cyt. pathway	0.911	-
+ aox	SDH	0.030	-0.045
state 4	NADH DH	0.071	-0.107
(B)	Cyt. pathway	0.684	1.115
	Alt. oxidase	0.216	-0.964

FIG. 5. **Effect of alternative oxidase expression on distribution of control under state 4 conditions in *S. pombe* mitochondria oxidizing succinate and NADH.** Curves representing state 4 kinetics of quinol-oxidizing pathways were taken from Fig. 2, *A* and *B*; the curve representing the combined kinetics of SDH and NADH DH was obtained by addition of curves taken from Fig. 3, *A* and *B* (*panel A*). Flux and flux ratio control coefficients (C^J and C^{rca}, respectively) of the respiratory enzymes (*panel B*) were calculated as described under "Experimental Procedures." Flux ratio refers to the quotient of the electron transfer rate through the cytochrome pathway and the alternative oxidase. *SDH*, succinate dehydrogenase; *NADH DH*, external-NADH dehydrogenase; *Cyt. pathway*, cytochrome pathway; *Alt. oxidase* = *aox*, alternative oxidase.

pression since growth on glucose is considerably less affected (Fig. 1, *A* and *B*). This paper is, to our knowledge, the first to report a phenotypic effect of alternative oxidase expression. Previously, plants have been genetically modified to yield a higher level of, *in vitro* active, alternative oxidase protein (18, 19). However, these plants were not phenotypically affected, possibly because of restricted engagement of the oxidase *in vivo*. The negative effect on *S. pombe* growth suggests that, in this system, the alternative oxidase is not merely expressed (*cf.* Ref. 14) but also contributes *in vivo* to the overall respiratory activity.

Analysis of mitochondrial respiratory kinetics strongly indicates that the alternative oxidase has indeed the potential to be engaged during *S. pombe* respiration. This is particularly evident from the alternative oxidase kinetics with respect to the Q-redox poise that suggest a relatively high affinity of the enzyme for QH_2 relative to Q (Fig. 2*B*). In plants, alternative oxidase activity is stimulated by pyruvate, mainly at low Q-redox levels (35). This apparently increased relative affinity for QH_2 enables the enzyme to compete for reducing equivalents with the cytochrome pathway (10). When the alternative oxidase kinetics in *S. pombe* are considered in relation to the kinetics of the other enzymes interacting with the Q-pool, the potential of the oxidase to actively compete for reducing equivalents is confirmed. MCA shows that the alternative oxidase exerts ~22% of the total control on overall electron flux during state 4 conditions, which is at the expense of the cytochrome path (Fig. 5). Furthermore, control of the alternative oxidase on the relative electron fluxes through the QH_2-oxidizing pathways is almost equal (in absolute terms) to that of the cytochrome pathway (Fig. 5). Kinetic modeling of the interaction between mitochondrial respiratory enzymes predicts that, in transformed *S. pombe*, ~20% of the total respiratory activity is accounted for by the alternative oxidase (Fig. 4).

From Fig. 2C it is apparent that the presence of a kinetically competent alternative oxidase results in decreased electron flow through the cytochrome pathway both under state 4 (at any Q-redox poise) and state 3 (at Q-redox levels > 30%) conditions. Since the uncoupled cytochrome pathway kinetics are not significantly affected, particularly at Q-reduction levels above 40% (Fig. 2), it is unlikely that the decreased state 4 and 3 activities are because of reduced expression levels of any one of the components of the cytochrome pathway. Instead, the competitive action of the alternative oxidase is likely to restrict

the amount of substrate (*i.e.* QH_2) available for the cytochrome bc_1 complex. Interestingly, not only the cytochrome pathway but also the total oxidative state 4 and 3 activities are affected by alternative oxidase expression (*cf.* Fig. 2, *A* and *B*). This suggests that the decrease in cytochrome pathway activity is not fully compensated for by alternative oxidase activity. This may be explained by the different capacities of the respective pathways.

The electron turnover capacity of the cytochrome pathway is measured as the specific oxygen consumption rate in mitochondria lacking the alternative oxidase (Fig. 2*A*). Under comparable conditions, the electron turnover capacity of the alternative pathway is measured as the specific antimycin-resistant oxygen uptake rate (Fig. 2*B*). It is evident that the total electron turnover capacity of the alternative oxidase is considerably lower than that of the cytochrome pathway under any energetic condition and at any Q-reduction level. This might be because of differences in protein levels and/or might be related to the minimum V_{max} values of the two pathways. The reported minimum V_{max} of the alternative oxidase is 186 electrons s^{-1} (34), which is approximately half the value reported for the yeast cytochrome bc_1 complex (36) and one-eighth of that reported for yeast cytochrome *c* oxidase (37). It is therefore tempting to speculate that alternative oxidase expression confers a respiratory pathway in *S. pombe* that transfers fewer electrons per second than the endogenous cytochrome pathway. When the availability of QH_2 for the latter pathway is restricted by the competitive action of the alternative oxidase, the overall rate of electron turnover is decreased.

The kinetic data shown in Figs. 2 and 3 are reasonably well described by the mathematical model developed by Van den Bergen and co-workers (9, 27, 29). This model, which assumes homogeneity of the Q-pool, has been successfully used to model mitochondrial respiratory kinetics in several plant systems (9, 31). *S. pombe* is therefore comparable with plants in that the core of its respiratory chain is formed by one homogeneous Q-pool that connects dehydrogenases with oxidases. However, the two systems differ in the way in which the kinetics of the cytochrome pathway are regulated by the protonmotive force. In plant mitochondria, a reduced protonmotive force results in strongly increased cytochrome pathway activity at any Q-reduction level (6, 7, 9, 10, 31). In contrast, cytochrome pathway activity in *S. pombe* is stimulated by a decreased protonmotive force only at high reduction levels of the Q-pool (Fig. 2*A*).

Although the effect of the protonmotive force in *S. pombe* mitochondria is not clearly understood, it appears that the electron transfer rate of the cytochrome pathway is increased upon uncoupling while the relative affinity for QH_2 is decreased. This may explain why the cytochrome pathway kinetics are less affected by alternative oxidase expression under uncoupled conditions than under state 4 or state 3 conditions. Although the mathematical fits do not differ significantly (Fig. 2*C*), the data in Fig. 2, *A* and *B* show that, at low Q-reduction levels (<40%), uncoupled oxygen uptake rates are higher in the absence than in the presence of the alternative oxidase. This suggests that the oxidase is only able to compete for reducing equivalents at a relatively low Q-redox poise. At higher Q-reduction levels, (>40%) cytochrome pathway activity is increased to such a degree that the contribution of the alternative oxidase to the overall rate becomes insignificant.

In conclusion, the results presented in this paper are the first to report a phenotypic effect because of the expression of the plant alternative oxidase. We suggest that the mechanisms which down-regulate the engagement of the alternative oxidase under physiological conditions in plants are non-operative in *S. pombe*. Consequently, the alternative oxidase is capable of contributing considerably to respiration under a variety of physiological conditions. Interestingly, such a contribution results in diminished mitochondrial oxygen consumption rates and, significantly, in a decreased overall efficiency of energy conservation. This has a distinct detrimental effect on yeast growth, particularly when cells are cultured on a non-fermentable carbon source.

Acknowledgment—We thank Dr. D. G. Whitehouse for critically reading the manuscript.

REFERENCES

1. Moore, A. L., and Siedow, J. N. (1991) *Biochim. Biophys. Acta* **1059,** 121–140
2. Vanlerberghe, G. C., and McIntosh, L. (1997) *Annu. Rev. Plant Physiol. Plant Mol. Biol.* **48,** 703–734
3. Siedow, J. N., and Umbach, A. L. (1995) *Plant Cell* **7,** 821–831
4. Day, D. A., Whelan, J., Millar, A. H., Siedow, J. N., and Wiskich, J. T. (1995) *Aust. J. Plant Physiol.* **22,** 497–509
5. Wagner, A. M., and Krab, K. (1995) *Physiol. Plant.* **95,** 318–325
6. Moore, A. L., Dry, I. B., and Wiskich, J. T. (1988) *FEBS Lett.* **235,** 76–80
7. Dry, I. B., Moore, A. L., Day, D. A., and Wiskich, J. T. (1989) *Arch. Biochem. Biophys.* **273,** 148–157
8. Siedow, J. N., and Moore, A. L. (1993) *Biochim. Biophys. Acta* **1142,** 165–174
9. Van den Bergen, C. W. M., Wagner, A. M., Krab, K., and Moore, A. L. (1994) *Eur. J. Biochem.* **226,** 1071–1078
10. Hoefnagel, M. H. N., Millar, A. H., Wiskich, J. T., and Day, D. A. (1995) *Arch. Biochem. Biophys.* **318,** 394–400
11. Umbach, A. L., and Siedow, J. N. (1993) *Plant Physiol.* **103,** 845–854
12. Moore, A. L., Umbach, A. L., and Siedow, J. N. (1995) *J. Bioenerg. Biomembr.* **27,** 367–377
13. Siedow, J. N., Umbach, A. L., and Moore, A. L. (1995) *FEBS Lett.* **362,** 10–14
14. Albury, M. S., Dudley, P., Watts, F. Z., and Moore, A. L. (1996) *J. Biol. Chem.* **271,** 17062–17066
15. Albury, M. S., Affourtit, C., and Moore, A. L. (1998) *J. Biol. Chem.* **273,** 30301–30305
16. Moore, A. L., Bonner, W. D., and Rich, P. R. (1978) *Arch. Biochem. Biophys.* **186,** 298–306
17. Moore, A. L., and Bonner, W. D. (1982) *Plant Physiol.* **70,** 1271–1276
18. Vanlerberghe, G. C., Vanlerberghe, A. E., and McIntosh, L. (1994) *Plant Physiol.* **106,** 1503–1510
19. Hiser, C., Kapranov, P., and McIntosh, L. (1996) *Plant Physiol.* **110,** 277–286
20. Moore, A. L., Walters, A. J., Thorpe, J., Fricaud, A. C., and Watts, F. Z. (1992) *Yeast* **8,** 923–933
21. Jault, J. M., Comte, J., Gautheron, D. C., and Dipietro, A. (1994) *J. Bioenerg. Biomembr.* **26,** 447–456
22. Murray, J. M., Carr, A. M., Lehmann, A. R., and Watts, F. Z. (1991) *Nucleic Acids Res.* **19,** 3525–3531
23. Okazaki, K., Okazaki, N., Kume, K., Jinno, S., Tanaka, K., and Okayama, H. (1990) *Nucleic Acids Res.* **18,** 6485–6489
24. Smith, P. K., Krohn, R. I., Hermanson, G. T., Mallia, A. K., Gartner, F. H., Provenzano, M. D., Fujimoto, E. K., Goeke, N. M., Olson, B. J., and Klenk, D. C. (1985) *Anal. Biochem.* **150,** 76–85
25. Fell, D. A. (1992) *Biochem. J.* **286,** 313–330
26. Brand, M. D. (1996) *J. Theor. Biol.* **182,** 351–360
27. Krab, K., Van den Bergen, C. W. M., and Moore, A. L. (1995) *Biochem. Soc. Trans.* **23**, S289
28. Moore, A. L., Leach, G., Whitehouse, D. G., van den Bergen, C. W. M., Wagner, A. M., and Krab, K. (1994) *Biochim. Biophys. Acta* **1187,** 145–151
29. Krab, K. (1995) *J. Bioenerg. Biomembr.* **27,** 387–396
30. Westerhoff, H. V., and Kell, D. B. (1987) *Biotechnol. Bioeng.* **30,** 101–107
31. Millar, A. H., Finnegan, P. M., Whelan, J., Drevon, J. J., and Day, D. A. (1997) *Plant Cell Environ.* **20,** 1273–1282
32. Gutman, M., Kearney, E. B., and Singer, T. P. (1971) *Biochemistry* **10,** 4763–4770
33. Oestreicher, G., Hogue, P., and Singer, T. P. (1973) *Plant Physiol.* **52,** 622–626
34. Hoefnagel, M. H. N., Wiskich, J. T., Madgwick, S. A., Patterson, Z., Oettmeier, W., and Rich, P. R. (1995) *Eur. J. Biochem.* **233,** 531–537
35. Umbach, A. L., Wiskich, J. T., and Siedow, J. N. (1994) *FEBS Lett.* **348,** 181–184
36. Ljungdahl, P. O., Pennoyer, J. D., and Trumpower, B. L. (1986) *Methods Enzymol.* **126,** 181–191
37. Geier, B. M., Schägger, H., Ortwein, C., Link, T. A., Hagen, W. R., Brandt, U., and Von Jagow, G. (1995) *Eur. J. Biochem.* **227,** 296–302